ORIGINAL RESEARCH

Faecal virome transplantation decreases symptoms of type 2 diabetes and obesity in a murine model

Torben Sølbeck Rasmussen ,[1] Caroline Märta Junker Mentzel,[2] Witold Kot,[3] Josué Leonardo Castro-Mejía,[1] Simone Zuffa,[4] Jonathan Richard Swann,[4] Lars Hestbjerg Hansen,[3] Finn Kvist Vogensen,[1] Axel Kornerup Hansen,[2] Dennis Sandris Nielsen[1]

► Additional material is published online only. To view, please visit the journal online (http://dx.doi.org/10.1136/gutjnl-2019-320005).

[1]Food Science, University of Copenhagen, Frederiksberg, Denmark
[2]Veterinary and Animal Sciences, University of Copenhagen, Frederiksberg, Denmark
[3]Plant and Environmental Sciences, University of Copenhagen, Frederiksberg, Denmark
[4]Metabolism, Digestion and Reproduction, Imperial College London, London, UK

Correspondence to
Mr Torben Sølbeck Rasmussen, Food Science, University of Copenhagen, Frederiksberg 1958, Denmark; torben@food.ku.dk
Dr Dennis Sandris Nielsen; dn@food.ku.dk

Received 4 October 2019
Revised 11 February 2020
Accepted 21 February 2020
Published Online First 12 March 2020

ABSTRACT

Objective Development of obesity and type 2 diabetes (T2D) are associated with gut microbiota (GM) changes. The gut viral community is predominated by bacteriophages (phages), which are viruses that attack bacteria in a host-specific manner. The antagonistic behaviour of phages has the potential to alter the GM. As a proof-of-concept, we demonstrate the efficacy of faecal virome transplantation (FVT) from lean donors for shifting the phenotype of obese mice into closer resemblance of lean mice.

Design The FVT consisted of viromes with distinct profiles extracted from the caecal content of mice from different vendors that were fed a low-fat (LF) diet for 14 weeks. Male C57BL/6NTac mice were divided into five groups: LF (as diet control), high-fat (HF) diet, HF+ampicillin (Amp), HF+Amp+FVT and HF+FVT. At weeks 6 and 7 of the study, the HF+FVT and HF+Amp+FVT mice were treated with FVT by oral gavage. The Amp groups were treated with Amp 24 hours prior to first FVT treatment.

Results Six weeks after first FVT, the HF+FVT mice showed a significant decrease in weight gain compared with the HF group. Further, glucose tolerance was comparable between the LF and HF+FVT mice, while the other HF groups all had impaired glucose tolerance. These observations were supported by significant shifts in GM composition, blood plasma metabolome and expression levels of genes associated with obesity and T2D development.

Conclusions Transfer of caecal viral communities from mice with a lean phenotype into mice with an obese phenotype led to reduced weight gain and normalised blood glucose parameters relative to lean mice. We hypothesise that this effect is mediated via FVT-induced GM changes.

Significance of this study

What is already known on this subject?
- Obesity and type 2 diabetes (T2D) are associated with gut microbiota (GM) dysbiosis.
- Faecal microbiota transplantion (FMT) from lean donors has previously shown potential in treating obesity and T2D.
- Patients suffering from recurrent *Clostridioides difficile* infections have been cured with sterile filtered donor faeces (containing enteric viruses and no bacteria), here defined as faecal virome transplantation (FVT).

What are the new findings?
- A decreased weight gain and a normalised blood glucose tolerance in a diet-induced obesity mouse modelwere observed following FVT from lean donors.
- FVT significantly changed the bacterial and viral GM component, as well as the plasma metabolome and the expression profiles of obesity and T2D-associated genes.
- Initial treatment with ampicillin prior to FVT seems to counteract the beneficial effects associated with FVT.

How might it impact on clinical practice in the foreseeable future?
- We here show a proof-of-concept experiment, providing a solid base for designing a clinical study of FVT targeting obesity and T2D in humans. This is further augmented by the removal of bacteria from the donor faeces during faecal virome preparation, which decreases the risk of invasive infections caused by bacteria.
- These findings highlight the potential application of FVT treatment of various diseases related to GM dysbiosis and further support the vital role of the viral community in maintaining and shaping the GM.

INTRODUCTION

Obesity and type 2 diabetes (T2D) constitute a worldwide health threat.[1] During the last decade, it has become evident that certain diseases, including obesity and T2D, are associated with gut microbiota (GM) dysbiosis.[2] Interestingly, germ-free (GF) mice do not develop diet-induced obesity (DIO),[3] but when exposed to faecal microbiota transplantation (FMT) from an obese human donor, they increase their body weight significantly more compared with GF mice exposed to FMT from a lean donor.[4] At present, FMT is widely used to efficiently treat recurrent *Clostridioides difficile* infections (rCDIs)[5] and is suggested to have therapeutic potential against metabolic syndrome, a condition related

Check for updates

To cite: Rasmussen TS, Mentzel CMJ, Kot W, *et al*. *Gut* 2020;**69**:2122–2130.

to obesity and T2D.[6] FMT is considered as a safe treatment, however, safety issues remain since screening methods cannot fully prevent adverse effects caused by disease transmission from the donor faeces.[7] A failure in the screening procedure caused recently the death (June 2019) of a patient following FMT[8] due to a bacterial infection.

The gut viral community (virome) is dominated by prokaryotic viruses,[9] also called bacteriophages (phages), which are viruses that attack bacteria in a host-specific manner.[10] During recent years, evidence has mounted that the gut virome plays a key role in shaping the composition of the GM[11 12] as well as influencing the host metabolome.[13] Intriguingly, rCDI have been treated by transfer of filtered donor faeces (containing phages, but no intact bacterial cells), which successfully eliminated rCDI symptoms for minimum 6 months in five out of five patients.[14] This approach is referred to as faecal virome transplantation (FVT). Also, antibiotic treatment alters the GM composition, but Draper *et al*. recently showed that the murine GM can be reshaped with FVT after antibiotic treatment.[15] Furthermore, a recent study took advantage of the antagonistic role of phages to efficiently target and decrease the abundance (in faeces) of cytolytic *Enterococcus faecalis* strains that are involved in alcoholic liver disease and thereby eased the symptoms of the recipient mice.[16]

DIO mice is a common animal model of metabolic syndrome, including symptoms such as obesity and insulin resistance/pre-T2D in male mice.[17] With C57BL/6NTac mice as the model, we hypothesised that FVT (originating from lean and healthy donor mice) treatment of DIO mice would change the GM composition and directly or indirectly counteract the symptoms of obesity and T2D. To the best of our knowledge, this is the first study investigating the effect of FVT targeting obesity and T2D.

METHODS

Detailed methods are enclosed in the online supplementary materials.

Animal study design

Forty male C57BL/6NTac mice (Taconic Biosciences A/S, Lille Skensved, Denmark) were divided into five groups at 5 weeks of age: low-fat (LF) diet (as lean control), high-fat (HF) diet, HF+ampicillin (Amp), HF+Amp+FVT and HF+FVT (figure 1). Only male C57BL/6NTac mice were included since female mice are protected against DIO.[18] For 13 weeks, mice were fed ad libitum a HF diet (Research Diets D12492, USA) or a LF diet (Research Diets D12450J, USA). After 6 weeks on their respective diets, the HF+FVT and HF+Amp+FVT mice were treated twice by FVT with 0.15 mL enteric virome by oral gavage with a 1-week interval (weeks 6 and 7) between the FVTs. On the day before the first FVT inoculation, the HF+Amp and HF+Amp+FVT animals were treated with a single dose of Amp (1 g/L) in the drinking water. The viromes used for FVT were extracted and mixed from the caecal content of 18 C57BL/6N mice representing three different vendors fed LF diet for 14 weeks. Mice from each individual vendor represented a unique and diverse viral profile.[19] The titre of the applied FVT virome was approximately 2×10^{10} virus-like particles/mL (online supplementary figure S1). The mice were subjected to an oral glucose tolerance test (OGTT)[20] at week 12 of the study, and food intake and mouse weight were monitored. The study was approved by the Danish Competent Authority, The Animal Experimentation Inspectorate, under the Ministry of Environment and Food of Denmark, and with license ID 2017-15-0201-01262 C1. Procedures were carried out in accordance with the Directive 2010/63/EU and the Danish law LBK Nr 726 af 09/091993, and housing conditions as earlier described.[19] Blood plasma, intestinal content from the caecum and colon, as well as tissue from the liver and ileum were sampled at termination at week 13 (18 weeks old). Mouse data (weight and OGTT levels) were analysed in GraphPad Prism using one-way analysis of variance with Tukey's post hoc test.

Preprocessing of faecal samples

This study included in total 79 intestinal content samples, of which 40 were isolated from the caecum and 39 from the colon. Preprocessing was performed as described earlier.[19]

Bacterial DNA extraction, sequencing and preprocessing of raw data

Tag-encoded 16S rRNA gene amplicon sequencing was performed on an Illumina NextSeq using V.2 MID output 2×150 cycles chemistry (Illumina, California, USA). DNA extraction and library building for amplicon sequencing was performed in

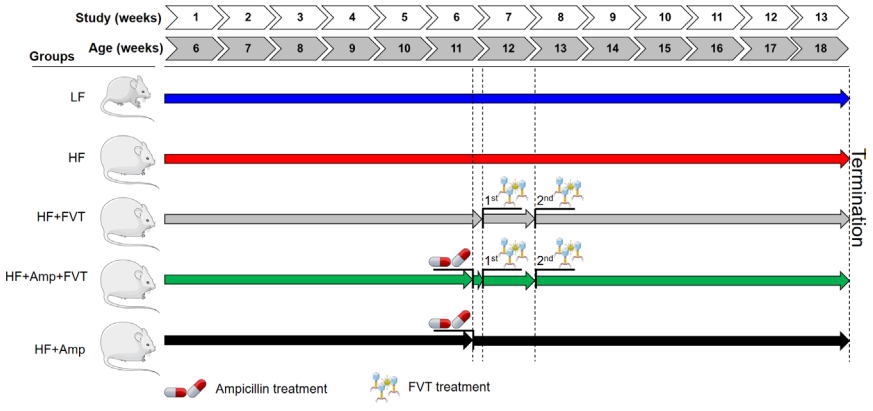

Figure 1 Experimental setup of the FVT. Forty male C57BL/6NTac mice (5 weeks old) were divided into five groups: LF diet (as lean control), HF diet, HF+Amp, HF+Amp+ FVT and HF+FVT. Their respective diets were provided continuously for 13 weeks until termination (18 weeks old). The HF+FVT and HF+Amp+ FVT mice were treated with FVT twice with 1-week interval by oral gavage at weeks 6 and 7 of the study. Amp was added once to the drinking water 1 day before first FVT (week 6) for the HF+Amp and HF+Amp+FVT mice. Icons originates from https://smart.servier.com/ and complies to Creative Commons Attribution 3.0 Unported (CC-BY) obligations . Amp, ampicillin; FVT, faecal virome transplantation; HF, high fat; LF, low fat.

accordance with Krych *et al*.[21] The average sequencing depth (accession: PRJEB32560, available at European Nucleotide Archive (ENA)) for the caecum 16S rRNA gene amplicons was 164 147 reads (minimum (min.) 22 732 reads and maximum (max.) 200 203 reads) and 166 012 reads for the colon (min. 89 528 reads and max. 207 924 reads) (online supplementary table S1). Bacterial operational taxonomic unit (bOTU) tables were generated and taxonomy assigned as earlier described.[19] The bacterial density of the caecal and colon content was estimated by quantitative PCR (qPCR) as previously described,[22] using the 16S rRNA gene primers (V3 region) also applied for the amplicon sequencing.[21]

Viral DNA extraction, sequencing and preprocessing of raw data

The enteric viral community was purified; DNA was extracted; and the gut metavirome was determined as previously described.[19] The average sequencing depth (accession: PRJEB32560, available at ENA) for the caecum viral metagenome was 612 640 reads/sample (min. 277 582 reads and max. 1 219 178 reads) and 356 976 reads/sample for colon (min. 33 773 reads and max. 584 681 reads) (online supplementary table S1). For each sample, reads were treated with Trimmomatic[23] and Usearch[24] and subjected to within-sample de novo assembly with MetaSpades .[25 26] Viral contigs were identified with Kraken2,[27] VirFinder,[28] PHASTER[29] and virus orthologous proteins (www.vogdb.org). Contaminations of non-viral contigs like bacteria, human, mice and plant DNA were removed, and the samples were screened for the presence of rRNA genes (online supplementary figure S2). The remaining contigs constituted the viral operational taxonomic unit (vOTU) table.

Gene expression assay

Genes investigated for expression analysis were selected based on relevant pathways for each tissue. For the liver, genes involved in metabolic pathways (triglyceride, carbohydrate, bile and cholesterol metabolism) and inflammation were selected. For the ileum, genes involved in inflammation, GM signalling and gut barrier function were selected.[30 31] Primer sequences are listed in online supplementary tables S2 and S3. qPCR was performed using the Biomark HD system (Fluidigm Corporation) on 2×96.96 integrated fluidic circuit (IFC) chips on preamplified cDNA duplicates following the instructions of the manufacturer with minor adjustments as previously described.[32] Gene expression data were analysed in R using linear models with either HF or LF as control groups. Eight tissue-specific reference genes were assessed in both the ileum and liver samples (see detailed description in the online supplementary materials).

Blood plasma metabolome analysis

Plasma samples were prepared for ultra performance liquid chromatography–mass spectrometry (UPLC-MS) analysis according to a previously published protocol.[33] Principal component analysis (PCA) and orthogonal projection to latent structures discriminant analysis (OPLS-DA) models were built on the plasma metabolic profiles to identify biochemical variation between the groups. Among the features driving the different OPLS-DA models, only those with variable importance in the projection (VIP) scores of >2 were further investigated. Putative annotation was achieved through searching for the m/z values in online databases such as HMDB (http://www.hmdb.ca), METLIN (http://metlin.scripps.edu) and Lipidmaps (http://www.lipidmaps.org). Additionally, fragmentation patterns derived from MS^e experiment were compared with online spectra when available.

Bioinformatic analysis of bacterial and viral DNAs

Prior to any analysis, the raw read counts in vOTU tables were normalised by reads per kilo base per million mapped reads (RPKM).[34] bOTUs and vOTUs that were detected in less than 8% of the samples were discarded to reduce noise while still maintaining an average total abundance close to 98%. Analysis of similarities (ANOSIM) and Kruskal-Wallis were used to evaluate multiple group comparisons. Regularised canonical correlation analysis (rCCA) was performed with mixOmics R package[35] to predict correlations between bacterial and viral taxa. Only vOTUs of ≥5000 bp were included in the rCCA. The machine learning algorithm random forest[36] was applied to select variables explaining the dataset and normalised in range of −1:1 ((x−mean)/max(abs(x−mean)) and visualised by Heatmap3.[37] Phage–host predictions were based on transfer RNA (tRNA) and clustered regularly interspaced short palindromic repeats (CRISPR) spacers.[38]

RESULTS

Here we investigated the potential of FVT to shift the phenotype of obesity and T2D in DIO male C57BL/6NTac mice towards a lean mice phenotype. Intestinal contents from the caecum and colon were isolated, but here only results from the caecum samples are reported. Complete equivalent analysis of colon samples can be found in online supplementary figure S3.

FVT from lean donor decreases weight gain and normalises blood glucose tolerance in DIO mice

Mice were weighed pre-FVT and post-FVT with 1–2 weeks of interval (see figure 1 for experimental setup). At both 4 and 6 weeks after first FVT (15 and 17 weeks old), a significantly lower body weight gain was observed in the HF+FVT ($p<0.017$) and the HF+Amp mice ($p<0.006$) compared with the HF mice (figure 2A). Intriguingly, OGTT showed no significant differences ($p>0.842$) between the LF and the HF+FVT mice, while the OGTT level of the HF mice was significantly increased ($p<0.0001$) compared with both the LF and HF+FVT group, suggesting that FVT had normalised the blood glucose tolerance in the HF+FVT mice (figure 2B). Furthermore, the OGTT of HF+Amp+FVT was comparable to the HF mice ($p>0.999$), indicating that the initial disruption of the bacterial composition by the Amp treatment had counteracted the effect of the FVT in the HF+Amp+FVT mice. This simultaneously suggest that the effects associated with the FVT occur via alterations in the GM component. Non-fasted blood glucose was measured regularly in addition to HbA1c levels for each mouse and food consumption per cage (online supplementary figure S4).

FVT enhances the expression of genes involved in whole-body energy homeostasis

Gene expression panels were designed to target genes relevant for obesity and T2D in liver and ileum tissue to measure if the expression of these genes in the HF+FVT mice were significantly different from the HF mice while being comparable with the LF mice. These conditions were represented by several genes involved in whole-body energy homeostasis (figure 3). Gene expression analysis suggested that FVT diminished the differences in gene expression caused by the HF diet, resulting in an expression profile closely resembling that of the healthy LF mice. The expression levels of leptin cytokine receptors

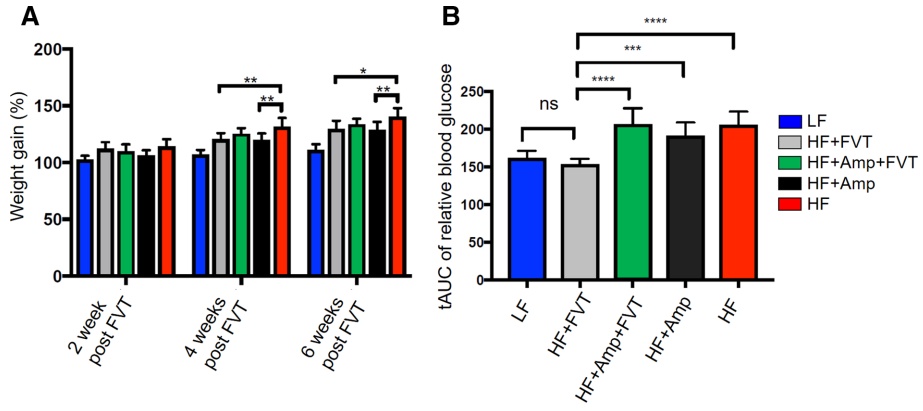

Figure 2 (A) Bar plot of body weight gain measured at 2, 4 and 6 weeks (13, 15 and 17 weeks old, respectively) after first FVT. (B) OGTT levels measured 6 weeks after first FVT (17 weeks old). Values are based on the tAUC relative to the blood glucose levels of the individual mouse. Significant differences of the pairwise comparison at weeks 4 and 6 after first FVT were excluded from the figures to increase the visualisation. *P<0.05, **P<0.006, ***P<0.0005, ****P< 0.0001. Amp, ampicillin; FVT, faecal virome transplantation; HF, high fat; LF, lowfat; ns, not significant; OGTT, oral glucose tolerance test; tAUC, total area under curve.

(*Lepr*^{Liver}) (leptin signalling), free fatty acid receptor (*Ffar2*^{Ileum}) (short chain fatty acid receptor), beta-klotho (*Klb*^{Liver}) (glucose metabolism), peroxisome proliferator-activated receptor gamma coactivator 1-alpha (*Ppargc1a*^{Liver}) (lipolysis and fatty acid oxidation) and insulin like growth factor binding protein (*Igfbp2*^{Liver}) (growth hormone) were significantly increased in the HF+FVT compared with the HF mice, whereas suppressor of cytokine signalling (*Socs3*^{Liver}) (leptin signalling) and transcription factor (*Myc*^{Liver}) were significantly decreased (figure 3). Generally, the gene expression levels (except *Socs3*^{Liver}) in the HF+FVT mice fell between the levels observed in the LF and HF mice, respectively. Significant differences (p<0.05) were observed in the expression of several other genes (57 of 74 for liver tissue and 58 of 74 for ileum tissue) between the experimental groups (see online supplementary table S4 for a complete list and associated pathways).

FVT-mediated shift in the GM component

At termination, the number of 16S rRNA gene copies/g of the caecum samples varied from 1.46×10^{10} to 2.70×10^{10} (online supplementary figure S5). The bacterial Shannon Diversity Index of the LF mice was significantly higher than that of the HF mice (p<0.005) but similar to that of the HF+FVT mice (p=0.816). The Shannon Diversity Index of the HF+FVT was likewise significantly increased (p<0.05) compared with that of the HF mice for caecum but not colon content (online supplementary figure S3). The Amp-treated HF+Amp mice had the lowest (p<0.002) Shannon Diversity Index of all groups at termination (ie, 7 weeks after treatment with Amp), and FVT increased the Shannon Diversity Index of Amp-treated HF+Amp+FVT mice (p<0.016) (figure 4A). FVT did not (p>0.59) impact the viral Shannon Diversity Index, whereas the Amp treatment

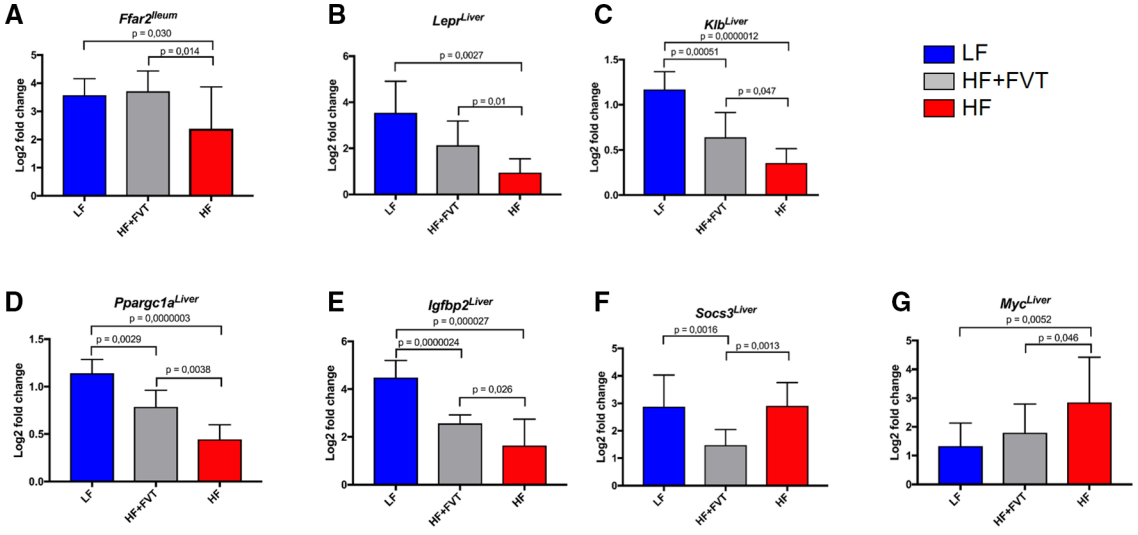

Figure 3 Gene expression levels at termination (18 weeks old) of (A) *Ffar2*^{Ileum} (B) *Lepr*^{Liver}, (C) *Klb*^{Liver}, (D) *Ppargc1a*^{Liver}, (E) *Igfbp2*^{Liver}, (F) *Socs3*^{Liver} and (G) *Myc*^{Liver}. Linear models with either HF or LF as control group was performed to calculate group significance. The log2 fold change is a measure of the relative gene expression and is based on log2 transformed expression values normalised to the sample with the lowest value. *Ffar2*^{Ileum}, free fatty acid receptor; *Igfbp2*^{Liver}, *insulin like growth factor binding protein; Klb*^{Liver}, beta-klotho; *Lepr*^{Liver}, leptin cytokine receptors; *Ppargc1a*^{Liver}, peroxisome proliferator-activated receptor gamma coactivator 1-alpha; *Socs3*^{Liver}, suppressor of cytokine signalling; *Myc*^{Liver}, transcription factor; FVT, faecal virome transplantation; HF, high fat; LF, lowfat; ns, not significant.

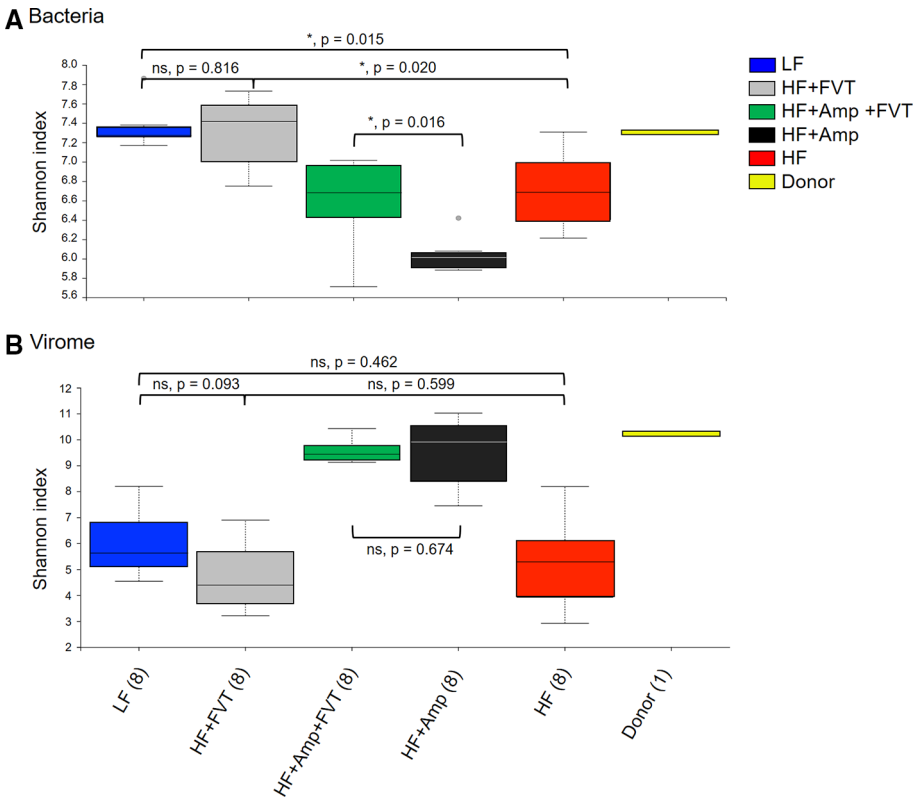

Figure 4 Shannon Diversity Index of the donor and caecal (A) bacterial and (B) viral community at termination (18 weeks old). The parentheses show the number of samples from each group included in the plot and grey dots indicate outliers. The donor is a 1:1:1 mix of bacteria or virome extracted from caecal content from three distinct donor profiles. Pairwise comparison of all groups can be found in online supplementary table S5. *P<0.05. Amp, ampicillin; FVT, faecal virome transplantation; HF, high fat; LF, low fat; ns, not significant.

significantly (p<0.003) increased the viral Shannon Diversity Index (figure 4B and online supplementary table S5), possibly due to induction of prophages (online supplementary figure S6).

The FVT strongly influenced both the bacterial (figure 5A, p<0.003) and viral (figure 5B, p<0.001) composition as determined by the Bray-Curtis dissimilarity metric, as illustrated by a clear separation of the HF+FVT compared with the HF mice and HF+Amp+FVT with the HF+Amp mice. The GM profile of the FVT recipients did not fully resemble the donor profile, which indicates that only parts of the donor virome was

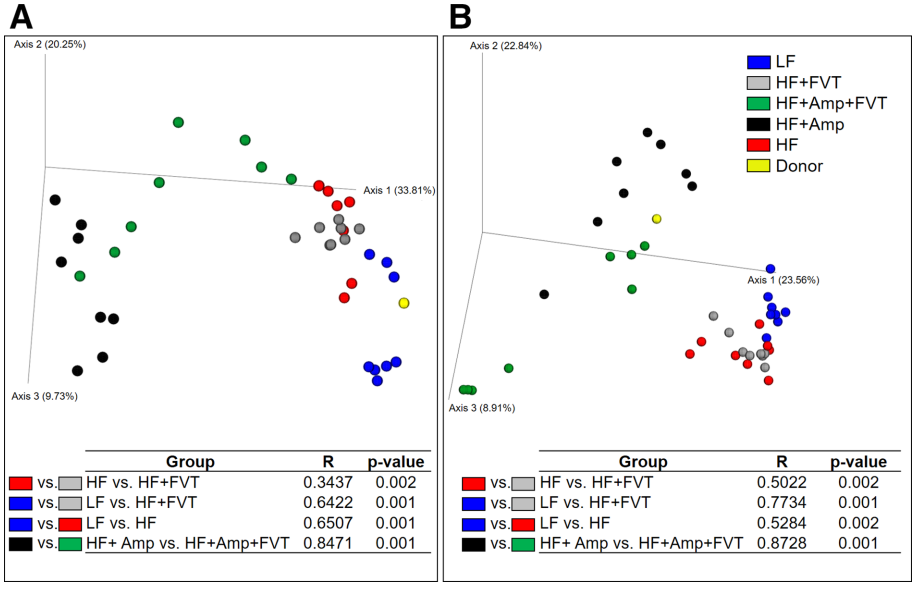

Figure 5 Principal coordinate analysis (PCoA) plots based on Bray-Curtis dissimilarity metric of the donor and caecal (A) bacterial community and (B) viral community at termination (18 weeks old). Analysis of similarities (ANOSIM) of the Bray-Curtis dissimilarity metrics is shown in tables. The donor is a 1:1:1 mix of bacteria or virome extracted from caecal content from three distinct donor profiles. Pairwise comparison of all groups can be found in online supplementary table S5. Amp, ampicillin; FVT, faecal virome transplantation; HF, high fat; LF, low fat.

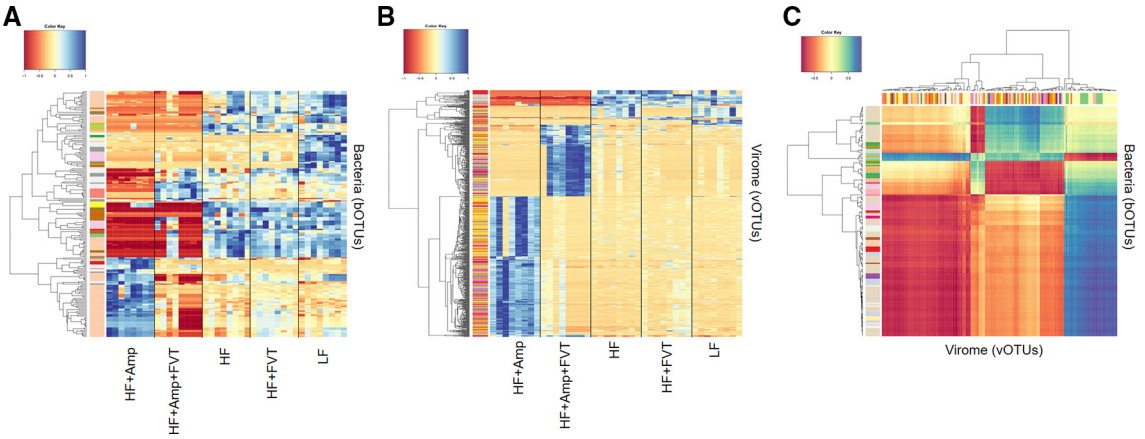

Figure 6 Heatmaps illustrating the bacterial (A) and viral (B) profile of all five experimental groups, as well as strong correlations between certain clusters of bacteria and viruses (C). Detailed information regarding OTU-associated taxonomy and high-resolution images can be found as supplemental materials, respectively, in online supplementary figures S7-S9. OTU, operational taxonomic unit.

established 6 weeks after inoculation. Further, all experimental groups were pairwise significantly separated ($p<0.003$) in both the viral and bacterial communities (online supplementary table S5), including LF versus HF+FVT ($p<0.001$). Overall, our findings suggest that FVT strongly influences and partly reshapes the GM composition both with and without Amp treatment. rCCA suggested potential host-phage pair relations by strong ($r>0.75$) positive and negative correlations between certain bacterial (order Bacteroidales and Clostridiales) and viral (order *Caudovirales*, family *Microviridae* and uncharacterised viruses) taxa. Likewise, random forest selected variables showed bacterial and viral coabundance profiles that differentiated the five experimental groups (see figure 6 and online supplementary figures S7-S9 for high-resolution images) supporting the effect of the FVT on the GM component.

Host-phage pair relations were also predicted, based on tRNA and CRISPR spacer databases (online supplementary figure S10). Relationships were observed between the predicted hosts and the actual abundance of four bacterial families: Desulfovibrionaceae, Bacteroidaceae, Lachnospiraceae and Rikenellaceae (constituting at least 70% of the total bacterial abundance). Interestingly, the Amp-treated mice had a clear increase in vOTUs predicted to target Desulfovibrionaceae compared with non-Amp-treated groups (online supplementary figure S10a), whereas the bacterial abundance of Desulfovibrionaceae was significantly ($p<0.05$) decreased (online supplementary figure S10e).

FVT-mediated shift in the blood plasma metabolome profile

The influence of FVT on host metabolome was determined by untargeted UPLC-MS analysis of plasma samples. A PCA model was built on a refined dataset comparing LF, HF and HF+FVT profiles (figure 7 and online supplementary figure S11 for all groups). Consistent with the other measures, the plasma profiles of HF+FVT mice were positioned between the HF and LF mice. Pairwise OPLS-DA models were constructed and all the models (LF versus HF, LF versus HF+FVT, HF versus HF+FVT) were significant ($p<0.025$), supporting the separation of the three groups. Among the selected features with a VIP score of >2, only those correlating with relevant gene expression (based on rCCA), and bacterial or viral abundance were further investigated for annotation. The features investigated consisted mainly of saturated and unsaturated lysophosphatidylcholine (LysoPC) and/or phosphatidylcholines (PCs), whereas the remaining features consisted of varieties of amino acids or unidentifiable metabolites (online supplementary table S6). Overall, the HF mice had higher levels of LysoPC (18:2), LysoPC (22:2), PC (16:0/22:6) and reduced plasma levels of LysoPC (22:4) and PC (18:1/O-18:2) compared with LF mice. The HF+FVT mice showed increased levels of circulating LysoPC (16:0), LysoPC (18:2) and PC (16:0/22:6) compared with the LF mice, while the levels of LysoPC (22:4) and PC (18:1/O-18:2) were decreased. Further, the HF+FVT mice appeared with higher levels of LysoPC (16:0), LysoPC (18:0) and PC (18:1/O-18:2) compared with the HF mice.

DISCUSSION

FVT has been successfully used to treat rCDI,[14] an effect probably mediated by the ability of FVT to reshape the GM of the recipient. However, several parameters differentiate obesity and T2D from rCDI, as this is a clonal infection highly susceptible to viral attack, a highly dysbiotic GM and the extensive use of antibiotics.[14] In a DIO mouse model, we here report that FVT originating from lean donors to obese recipients counteracts some of

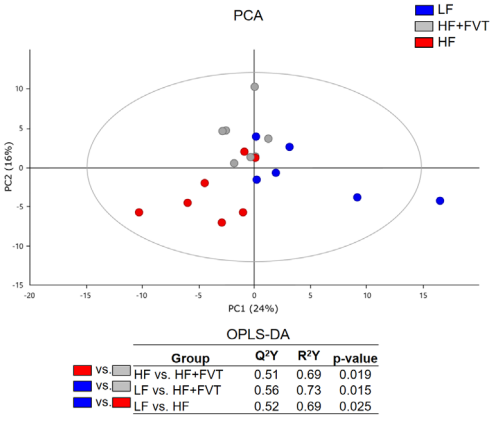

Figure 7 PCA score plot obtained from electrospray ionization (ESI) + UPLC-MS of plasma from LF, HF and HF+FVT (R2=0.40 and Q2=0.11) at termination (18 weeks old). Table includes supervised OPLS-DA models generated by pairwise comparisons. HF, high fat; LF, low fat; OPLS-DA, orthogonal projection to latent structures discriminant analysis; PCA, principal component analysis. UPLC-MS, ultraperformance liquid chromatography–mass spectrometry.

the adverse effects of a HF diet with a decrease in body weight gain ($p<0.0034$) and a normalised blood glucose tolerance relative to mice fed a LF diet. Of note, while we here show that FVT from lean donors positively influences the recipient phenotype, it cannot be ruled out that a transfer of virome from an obese donor (or other donor phenotypes) could cause similar changes in the recipient phenotype as those observed here.

Indeed, HF+FVT mice showed the same response in OGTT as the LF mice ($p>0.842$, figure 2), whereas similar effects were not observed in the HF+Amp+FVT mice. Induction of prophages, triggered by the Amp treatment, might have affected the OGTT response of HF+Amp+FVT mice via community shuffling[39] and by elevating phage abundance to an extent which might trigger inflammation[40] via toll-like receptor 9 (TLR9) and interferon-γ expression.[41] Further, the HF+Amp group appeared with a lower ($p<0.006$) weight gain, which would be in accordance to previous studies using high doses of antibiotics in mice.[42] It should be noted that the LF, HF and HF+Amp mice were not subjected to oral gavage containing the carrier solution during the FVT procedure and have thereby not been subjected to identical stressors as the HF+FVT and HF+Amp+FVT mice. However, several independent studies report that oral gavage in rodents has no clear long-term effects on various stress parameters[43–46]; thus, it is unlikely that the stressors associated with handling and oral gavage have affected the OGTT levels 6 weeks after the last FVT procedure. Furthermore, the HF+FVT and HF+Amp+FVT mice both underwent oral gavage, and the HF+Amp+FVT group did not have an altered response in OGTT compared with the HF control group.

As expected,[47] the Shannon Diversity Index of the caecal bacterial community in the HF mice was significantly ($p<0.005$) lower compared with that of the LF mice, but interestingly, the bacterial diversity of the HF+FVT was similar to that of the LF ($p>0.81$) and elevated in comparison ($p<0.015$) with the HF mice. No significant differences in viral Shannon Diversity Index measures were observed between LF versus HF, LF versus HF+FVT and HF versus HF+FVT. The significantly increased ($p<0.003$) diversity of the viral community in the Amp-treated mice (figure 4B and online supplementary table S5) was likely due to induction of prophages,[48] as indicated by an increased ($p<0.05$) presence of viral contigs containing integrase genes in the Amp-treated groups (online supplementary figure S6).

The composition of the viral community was dominated by order *Caudovirales* and family *Microviridae* viruses, which is in accordance with former studies investigating the enteric viral community in mammals.[9 11] The application of multiple displacement amplification (MDA) favours single-stranded DNA (ssDNA) viruses like *Microviridae*[49]; hence, this might have influenced the relative abundance of *Microviridae*. However, MDA was shortened to 30 min to minimise this effect. The FVT strongly influenced both the bacterial and viral GM composition (figure 5), with HF+FVT being significantly ($p<0.003$) different from both the HF as well as the LF mice. The highly diverse donor virome,[19] as well as the distinct nutrition profiles (HF diet versus LF diet), most likely explains the divergence in the GM composition profiles between the HF+FVT and the LF mice. Cage effects in murine models are a common issue[50 51] and are to some extent also observed when analysing the GM composition for especially the Amp-treated mice (online supplementary figure S12). However, no cage effect was observed for the measured phenotypic parameters (eg, weight gain and OGTT) of non-Amp-treated mice (online supplementary table S7).

Gene expression analysis of liver and ileum tissue showed that seven genes involved in among other leptin signalling, glucose metabolism and lipolysis (figure 3) were differentially expressed ($p<0.05$) between HF+FVT and HF mice and thereby further substantiate that FVT positively affected the glucose tolerance and weight gain. The *Ffar2* gene is involved in energy homeostasis and can influence glucose homeostasis through GLP-1 regulation and leptin production,[52 53] which might lower food intake and via GLP-1 decrease blood glucose levels by enhancing the production of insulin.[52] The *Ffar2* gene may also influence whole-body homeostasis through regulation of adipogenesis and lipid storage of adipocytes.[54] The expression of $Ffar2^{Ileum}$ was comparable between LF and HF+FVT, while in the HF mice, expression was clearly reduced (figure 3A). The *Lepr* genes are involved in the regulation of food intake, and *Lepr*-deficient subjects rapidly increase body weight.[55] *Klb* contributes to the repression of cholesterol 7-alpha-hydroxylase and thereby regulates bile acid synthesis[56] with reduced expression in obese subjects.[57] *Ppargc1a* expression has been reported to be reduced and linked with islet insulin secretion in patients with T2D,[58] as well as to play a pivotal role in regulating energy homeostasis.[59] *Igfbp2* is involved in the insulin-like growth factor axis influencing cell growth and proliferation,[60] and high expression levels have been linked to the protection against T2D in human studies.[61] The gene expressions of $Lepr^{Liver}$ (figure 3B), Klb^{Liver} (figure 3C), $Ppargc1a^{Liver}$ (figure 3D) and $Igfbp2^{Liver}$ (figure 3E) were all significantly increased in the LF and HF+FVT mice compared with the HF mice. Knockout of *Socs* genes has been reported to prevent insulin resistance in obesity as the result of a decrease in ceramide synthesis.[62] The $Socs3^{Liver}$ levels were significantly ($p<0.0001$) decreased in HF+FVT compared with both HF and LF mice (figure 3F). However, the overall $Socs3^{Liver}$ levels in the LF mice were affected by high intergroup variation. The expression of *Myc* has been found to be increased in mice provided HF diet, and a decrease in body weight was obtained with haploinsufficient mice ($c\text{-}Myc^{+/-}$).[63] The expression of Myc^{Liver} was comparable between LF and HF+FVT, while in the HF mice expression was clearly increased (figure 3G). Overall, these findings indicate that FVT treatment affects the expression of genes involved in controlling appetite, blood glucose tolerance and whole-body energy homeostasis.

An extensive study of metabolic syndrome in humans showed strong correlations between certain blood plasma metabolites and the GM component, and some of these correlations appear specific to the pre-diabetic state.[64] The blood plasma metabolome profile of the HF+FVT mice differed significantly ($p<0.025$) from both the LF and HF mice. Short-chain fatty acids (SCFA) are expected to regulate the *Ffar2* gene,[65] but our feature annotation did not detect any clear differences in circulating SCFAs between treatment groups. Further, LysoPCs are reduced in obesity and T2D,[66] and we indeed observed a decrease in LysoPCs levels when comparing the HF with the HF+FVT group and HF with the LF group, although the results were not clear.

Zuo *et al*.[67] investigated how the phage community could be related to the effect of FMT against rCDI and found that a few patients did not respond to the treatment. The common denominator of the patients that did respond on the FMT treatment was that the *Caudovirales* richness in the donor faeces was higher than the *Caudovirales* richness in the recipient, whereas most of the non-responder recipients had a higher Caudovirales richness than the donor. Based on these findings, Zuo *et al* hypothesised that a higher *Caudovirales* richness in the donor compared with the recipient is important for a successful FMT treatment.[67] In comparison to our study it should be noted that the viral dataset in Zuo *et al*.[67] was based on assembly of viral contigs from solely viral reference proteins which exclude the viral dark matter,[68] and the viral DNA was amplified for 2 hours instead of 30 min, which might increase the bias towards ssDNA vira associated

with MDA.[49] Interestingly, Park *et al* independently reported that viral diversity plays a role in the relative success of FMT.[69] The Caudovirales richness of the FVT donor virome in our study was higher than any of the recipient groups at termination (online supplementary figure S13). Whereas the Caudovirales richness of the viromes from the individual mouse vendors was notably less compared with the FVT virome and both recipient groups. These findings are consistent with those of Zuo *et al*.[67] and Park *et al*.[69] and suggests that a virome from a single vendor/donor might not have the same effect as when multiple viromes are combined for FVT.

We hypothesise that phages transferred with the FVT in the HF+FVT mice have reshaped the GM component and thereby shifted the phenotype of the obese HF mice to be in closer resemblance of the donor mice. This hypothesis seems plausible since several recent studies have reported a correlation between phage diversity and intestinal microbiome diversity,[11] an FVT-mediated restoration of the GM of antibiotic-treated mice[15] and a phage-mediated shift in the gut metabolome profile,[13] and finally, Lin *et al* showed how FVT from obese C57BL/6N donor mice could reshape the GM of lean LF recipient mice towards the GM composition of the obese donors.[70]

In conclusion, we demonstrate here the use of FVT targeting obesity and T2D in an animal model. Although the study is a proof-of-concept, our findings highlight the potential of using phage-mediated therapy against obesity and T2D that represents a worldwide health threat.[1]

Twitter Simone Zuffa @simonezuffa

Acknowledgements Thanks to Julie Mou Larsen for assisting with sampling of mouse tissue and associated method description. In addition, we thank Helene Farlov, Mette Nelander at Section of Experimental Animal Models and Liv de Vries at Section for Microbiology and Fermentation (University of Copenhagen, Denmark) for taking care of the animals. We thank Helle Keinicke and Marina Kjærgaard Gerstenberg for selecting the genes and providing the primers for the liver gene expression panel. The initial version of the manuscript was posted as a preprint on bioRxiv (doi.org/10.1101/792556).

Contributors TSR, CMJM, AKH, DSN and FKV conceived the research idea and designed the study; CMJM and TSR performed the animal experiments; TSR, CMJM and SZ processed the samples in the laboratory; TSR, CMJM, LHH, WK, DSN, JRS, SZ, JLC-M and FKV performed data analysis; TSR and DSN were responsible for the first and final drafts of the manuscript, as well as all requested revisions. All authors critically revised and approved the final version of the manuscript.

Funding Funding was provided by the Danish Council for Independent Research (grant ID: DFF-6111-00316) (PhageGut) and the Danish Innovation Fund project (7076-00129B), MICROHEALTH.

Competing interests None declared.

Patient and public involvement Patients and/or the public were not involved in the design, or conduct, or reporting, or dissemination plans of this research.

Patient consent for publication Not required.

Provenance and peer review Not commissioned; externally peer reviewed.

Data availability statement Data are available in a public open access repository. All data relevant to the study are included in the article or uploaded as supplementary information. Raw DNA sequencing data is available at European Nucleotide Archive (ENA) with accession PRJEB32560 (https://www.ebi.ac.uk/ena/data/view/PRJEB32560). The data includes raw demultiplexed Illumina sequencing reads of 16S rRNA amplicons and metaviromes. The remaining data sheets are available upon reasonable request.

ORCID iD
Torben Sølbeck Rasmussen http://orcid.org/0000-0002-9907-8953

REFERENCES

1 Leitner DR, Frühbeck G, Yumuk V, *et al*. Obesity and type 2 diabetes: Two diseases with a need for combined treatment strategies - EASO can lead the way. *Obes Facts* 2017;10:483–92.
2 Maruvada P, Leone V, Kaplan LM, *et al*. The human microbiome and obesity: moving beyond associations. *Cell Host Microbe* 2017;22:589–99.
3 Bäckhed F, Manchester JK, Semenkovich CF, *et al*. Mechanisms underlying the resistance to diet-induced obesity in germ-free mice. *Proc Natl Acad Sci U S A* 2007;104:979–84.
4 Ridaura VK, Faith JJ, Rey FE, *et al*. Gut microbiota from twins discordant for obesity modulate metabolism in mice. *Science* 2013;341:1241214.
5 Kelly CR, Kahn S, Kashyap P, *et al*. Update on fecal microbiota transplantation 2015: indications, methodologies, mechanisms, and outlook. *Gastroenterology* 2015;149:223–37.
6 Gupta S, Allen-Vercoe E, Petrof EO. Fecal microbiota transplantation: in perspective. *Therap Adv Gastroenterol* 2016;9:229–39.
7 Wang J-W, Kuo C-H, Kuo F-C, *et al*. Fecal microbiota transplantation: review and update. *J Formos Med Assoc* 2019;118 Suppl 1:S23–31.
8 FDA. FDA - Important Safety Alert Regarding Use of Fecal Microbiota for Transplantation and Risk of Serious Adverse Reactions Due to Transmission of Multi-Drug Resistant Organisms, 2019. Available: https://www.fda.gov/vaccines-blood-biologics/safety-availability-biologics/important-safety-alert-regarding-use-fecal-microbiota-transplantation-and-risk-serious-adverse [Accessed 4 Jul 2019].
9 Reyes A, Haynes M, Hanson N, *et al*. Viruses in the faecal microbiota of monozygotic twins and their mothers. *Nature* 2010;466:334–8.
10 Ross A, Ward S, Hyman P. More is better: selecting for broad host range bacteriophages. *Front Microbiol* 2016;7:1–6.
11 Moreno-Gallego JL, Chou S-P, Di Rienzi SC, *et al*. Virome diversity correlates with intestinal microbiome diversity in adult monozygotic twins. *Cell Host Microbe* 2019;25:261–72.
12 Howe A, Ringus DL, Williams RJ, *et al*. Divergent responses of viral and bacterial communities in the gut microbiome to dietary disturbances in mice. *Isme J* 2016;10:1217–27.
13 Hsu BB, Gibson TE, Yeliseyev V, *et al*. Dynamic modulation of the gut microbiota and metabolome by bacteriophages in a mouse model. *Cell Host Microbe* 2019;25:803–14.
14 Ott SJ, Waetzig GH, Rehman A, *et al*. Efficacy of sterile fecal filtrate transfer for treating patients with Clostridium difficile infection. *Gastroenterology* 2017;152:799–811.
15 Draper LA, Ryan FJ, Dalmasso M, *et al*. Autochthonous faecal virome transplantation (FVT) reshapes the murine microbiome after antibiotic perturbation. *bioRxiv* 2019;591099.
16 Duan Y, Llorente C, Lang S, *et al*. Bacteriophage targeting of gut bacterium attenuates alcoholic liver disease. *Nature* 2019;575:505–11.
17 Fraulob JC, Ogg-Diamantino R, Fernandes-Santos C, *et al*. A mouse model of metabolic syndrome: insulin resistance, fatty liver and non-alcoholic fatty pancreas disease (NAFPD) in C57BL/6 mice fed a high fat diet. *J Clin Biochem Nutr* 2010;46:212–23.
18 Pettersson US, Waldén TB, Carlsson P-O, *et al*. Female mice are protected against high-fat diet induced metabolic syndrome and increase the regulatory T cell population in adipose tissue. *PLoS One* 2012;7:e46057.
19 Rasmussen TS, de Vries L, Kot W, *et al*. Mouse vendor influence on the bacterial and viral gut composition exceeds the effect of diet. *Viruses* 2019;11:435.
20 Rune I, Rolin B, Lykkesfeldt J, *et al*. Long-Term Western diet fed apolipoprotein E-deficient rats exhibit only modest early atherosclerotic characteristics. *Sci Rep* 2018;8:1–12.
21 ł Krych, Kot W, Bendtsen KMB, *et al*. Have you tried spermine ? A rapid and cost-e ff ective method to eliminate dextran sodium sulfate inhibition of PCR and RT-PCR. *J Microbiol Methods J* 2018;144:1–7.
22 Ellekilde M, Krych L, Hansen CHF, *et al*. Characterization of the gut microbiota in leptin deficient obese mice - Correlation to inflammatory and diabetic parameters. *Res Vet Sci* 2014;96:241–50.
23 Bolger AM, Lohse M, Usadel B. Trimmomatic: a flexible trimmer for Illumina sequence data. *Bioinformatics* 2014;30:2114–20.
24 Edgar RC. UPARSE: highly accurate otu sequences from microbial amplicon reads. *Nat Methods* 2013;10:996–8.
25 Bankevich A, Nurk S, Antipov D, *et al*. SPAdes: a new genome assembly algorithm and its applications to single-cell sequencing. *J Comput Biol* 2012;19:455–77.
26 Nurk S, Meleshko D, Korobeynikov A, *et al*. metaSPAdes: a new versatile metagenomic assembler. *Genome Res* 2017;27:824–34.
27 Wood DE, Salzberg SL. Kraken: ultrafast metagenomic sequence classification using exact alignments. *Genome Biol* 2014;15:R46.
28 Ren J, Ahlgren NA, Lu YY, *et al*. VirFinder: a novel k-mer based tool for identifying viral sequences from assembled metagenomic data. *Microbiome* 2017;5:69.
29 Arndt D, Grant JR, Marcu A, *et al*. PHASTER: a better, faster version of the PHAST phage search tool. *Nucleic Acids Res* 2016;44:W16–21.
30 Bendtsen KM, Hansen CHF, Krych Łukasz, *et al*. Immunological effects of reduced mucosal integrity in the early life of BALB/c mice. *PLoS One* 2017;12:e0176662–20.
31 Zachariassen LF, Krych L, Rasmussen SH, *et al*. Cesarean section induces Microbiota-Regulated immune disturbances in C57BL/6 mice. *J Immunol* 2019;202:142–50.
32 Mentzel CMJ, Cardoso TF, Pipper CB, *et al*. Deregulation of obesity-relevant genes is associated with progression in BMI and the amount of adipose tissue in pigs. *Mol Genet Genomics* 2018;293:129–36.

33 Sarafian MH, Gaudin M, Lewis MR, *et al*. Objective set of criteria for optimization of sample preparation procedures for ultra-high throughput untargeted blood plasma lipid profiling by ultra performance liquid chromatography-mass spectrometry. *Anal Chem* 2014;86:5766–74.
34 Roux S, Emerson JB, Eloe-Fadrosh EA, *et al*. Benchmarking viromics: an *in silico* evaluation of metagenome-enabled estimates of viral community composition and diversity. *PeerJ* 2017;5:e3817.
35 Rohart F, Gautier B, Singh A, *et al*. mixOmics: An R package for 'omics feature selection and multiple data integration. *PLoS Comput Biol* 2017;13:e1005752.
36 Breiman L. Random forests. *Mach Learn* 2001;45:5–32.
37 Zhao S, Guo Y, Sheng Q, *et al*. Heatmap3: an improved heatmap package with more powerful and convenient features. *BMC Bioinformatics* 2014;15:P16.
38 Pasolli E, Asnicar F, Manara S, *et al*. Extensive unexplored human microbiome diversity revealed by over 150,000 genomes from metagenomes spanning age, geography, and lifestyle. *Cell* 2019;176:e20:649–62.
39 De Paepe M, Leclerc M, Tinsley CR, *et al*. Bacteriophages: an underestimated role in human and animal health? *Front Cell Infect Microbiol* 2014;4:1–11.
40 Norman JM, Handley SA, Baldridge MT, *et al*. Disease-Specific alterations in the enteric virome in inflammatory bowel disease. *Cell* 2015;160:447–60.
41 Gogokhia L, Buhrke K, Bell R, *et al*. Expansion of bacteriophages is linked to aggravated intestinal inflammation and colitis. *Cell Host Microbe* 2019;25:285–99.
42 Cox LM. Antibiotics shape microbiota and weight gain across the animal Kingdom. *Anim Front* 2016;6:8–14.
43 Alban L, Dahl PJ, Hansen AK, *et al*. The welfare impact of increased Gavaging doses in rats. *Animal welfare* 2001;10:303–14.
44 Bonnichsen M, Dragsted N, Hansen AK. The welfare impact of gavaging laboratory rats. *Anim Welf* 2005;14:223–7.
45 Arantes-Rodrigues R, Henriques A, Pinto-Leite R, *et al*. The effects of repeated oral gavage on the health of male CD-1 mice. *Lab Anim* 2012;41:129–34.
46 Jones CP, Boyd KL, Wallace JM. Evaluation of mice undergoing serial oral gavage while awake or anesthetized. *J Am Assoc Lab Anim Sci* 2016;55:805–10.
47 Sun L, Ma L, Ma Y, *et al*. Insights into the role of gut microbiota in obesity: pathogenesis, mechanisms, and therapeutic perspectives. *Protein Cell* 2018;9:397–403.
48 Allen HK, Looft T, Bayles DO, *et al*. Antibiotics in feed induce prophages in swine fecal microbiomes. *mBio* 2011;2:1–9.
49 Marine R, McCarren C, Vorrasane V, *et al*. Caught in the middle with multiple displacement amplification: the myth of pooling for avoiding multiple displacement amplification bias in a metagenome. *Microbiome* 2014;2:3.
50 Miyoshi J, Leone V, Nobutani K, *et al*. Minimizing confounders and increasing data quality in murine models for studies of the gut microbiome. *PeerJ* 2018;6:e5166.
51 Lundberg R, Bahl MI, Licht TR, *et al*. Microbiota composition of simultaneously colonized mice housed under either a gnotobiotic isolator or individually ventilated cage regime. *Sci Rep* 2017;7:1–11.
52 Hudson BD, Due-Hansen ME, Christiansen E, *et al*. Defining the molecular basis for the first potent and selective orthosteric agonists of the FFA2 free fatty acid receptor. *J Biol Chem* 2013;288:17296–312.
53 Ichimura A, Hasegawa S, Kasubuchi M, *et al*. Free fatty acid receptors as therapeutic targets for the treatment of diabetes. *Front Pharmacol* 2014;5:1–6.
54 Brown AJ, Goldsworthy SM, Barnes AA, Murdock PR, Pike NB, Eilert MM, *et al*. The orphan G protein-coupled receptors GPR41 and GPR43 are activated by propionate and other short chain carboxylic acids. *J Biol Chem* 2003;278:11312–9.
55 Dubern B, Clement K. Leptin and leptin receptor-related monogenic obesity. *Biochimie* 2012;94:2111–5.
56 Ito S, Fujimori T, Furuya A, *et al*. Impaired negative feedback suppression of bile acid synthesis in mice lacking betaKlotho. *J Clin Invest* 2005;115:2202–8.
57 Kruse R, Vienberg SG, Vind BF, *et al*. Effects of insulin and exercise training on FGF21, its receptors and target genes in obesity and type 2 diabetes. *Diabetologia* 2017;60:2042–51.
58 Ling C, Del Guerra S, Lupi R, *et al*. Epigenetic regulation of PPARGC1A in human type 2 diabetic islets and effect on insulin secretion. *Diabetologia* 2008;51:615–22.
59 Charos AE, Reed BD, Raha D, *et al*. A highly integrated and complex PPARGC1A transcription factor binding network in HepG2 cells. *Genome Res* 2012;22:1668–79.
60 Rajpathak SN, Gunter MJ, Wylie-Rosett J, *et al*. The role of insulin-like growth factor-I and its binding proteins in glucose homeostasis and type 2 diabetes. *Diabetes Metab Res Rev* 2009;25:3–12.
61 Wittenbecher C, Ouni M, Kuxhaus O, *et al*. Insulin-Like growth factor binding protein 2 (IGFBP-2) and the risk of developing type 2 diabetes. *Diabetes* 2019;68:188–97.
62 Yang G, Badeanlou L, Bielawski J, *et al*. Central role of ceramide biosynthesis in body weight regulation, energy metabolism, and the metabolic syndrome. *Am J Physiol Endocrinol Metab* 2009;297:E211–24.
63 Liu S, Kim T-H, Franklin DA, *et al*. Protection against High-Fat-Diet-Induced Obesity in $MDM2^{C305F}$ Mice Due to Reduced p53 Activity and Enhanced Energy Expenditure. *Cell Rep* 2017;18:1005–18.
64 Blum Y, Kasela S. Relationships between gut microbiota, plasma metabolites, and metabolic syndrome traits in the METSIM cohort. *Genome Biol* 2017;18:1–14.
65 Le Poul E, Loison C, Struyf S, *et al*. Functional characterization of human receptors for short chain fatty acids and their role in polymorphonuclear cell activation. *J Biol Chem* 2003;278:25481–9.
66 Barber MN, Risis S, Yang C, *et al*. Plasma lysophosphatidylcholine levels are reduced in obesity and type 2 diabetes. *PLoS One* 2012;7:e41456–12.
67 Zuo T, Wong SH, Lam K, *et al*. Bacteriophage transfer during faecal microbiota transplantation in *Clostridium difficile* infection is associated with treatment outcome. *Gut* 2018;67:634–43.
68 Roux S, Hallam SJ, Woyke T, *et al*. Viral dark matter and virus–host interactions resolved from publicly available microbial genomes. *eLife* 2015;4:e08490.
69 Park H, Laffin MR, Jovel J, *et al*. The success of fecal microbial transplantation in *Clostridium difficile* infection correlates with bacteriophage relative abundance in the donor: a retrospective cohort study. *Gut Microbes* 2019;10:676–87.
70 Lin DM, Koskella B, Ritz NL, *et al*. Transplanting fecal virus-like particles reduces high-fat diet-induced small intestinal bacterial overgrowth in mice. *Front Cell Infect Microbiol* 2019;9:1–11.